Journal of Marine Science and Technology
DOI: 10.6119/JMST-012-0904-1

This article has been peer reviewed and accepted for publication in JMST but has not yet been copyediting, typesetting, pagination and proofreading process. Please note that the publication version of this article may be different from this version. This article now can be cited as doi: 10.6119/JMST-012-0904-1.

NUMERICAL STABILITY ANALYSIS FOR INDEPENDENT MODAL VIBRATION SUPPRESSION OF A FLUID-CONVEYING PIPE USING A PIEZOELECTRIC INERTIA ACTUATOR

Yih-Hwang Lin [1], Jui-Lung Chen [2], Chih-Liang Chu [3], and Yau-Kun Tsai [4]

Keywords: independent modal space control, pipes conveying fluid, stability.

ABSTRACT

This study deals with numerical stability analysis for independent modal vibration suppression of a fluid-conveying pipe using a piezoelectric inertia actuator (PIA). The stability issue of the approach as proposed by the pioneer developers is addressed. The approach utilizes an infinite control weight for one component of the modal control input and results in a severe control spillover problem for the complex mode controlled, easily leading to closed loop instability even for open loop stable systems. The stability of the system depends on how the left eigenvector is normalized for transforming the original coupled equations to the decoupled ones in the modal space. A novel approach by rotating the left eigenvector on the complex plane is systematically examined to define the region of stability in this work. A feasible modal control design for systems possessing complex modes can thus be accomplished using the proposed approach.

I. INTRODUCTION

Smart actuators and intelligent structures receive a considerable interest in the field of active vibration suppression of structural systems. The associated stability issue for any vibration control strategy is crucial and must be fully examined to ensure successful deployment of smart structural systems. When compared to the traditional coupled mode control, the independent modal space control (IMSC) has been notable for its attractive features, such as far less computation time and storage requirements, which can be vital for real time control of high dimensional structures [18]. The control technique has been shown to be robust to parameter variations and versatile for selection of control approaches, including nonlinear control [15-17, 19]. Lin and Chu [12] reported a new design strategy for the independent modal space control of general dynamic systems with complex modes. The stability of the control system can be guaranteed under certain conditions. Lin, et al. [13] reported an optimal modal control approach for vibration suppression of a fluid-conveying pipe with a divergent mode. For the first time in the literature, the severe control spillover problem in the complex mode controlled when using the approach proposed by the pioneer developers of IMSC has been demonstrated experimentally [3]. The micro-vibration control of a smart flexible beam mounted on an elastic base was used to serve as a test case.

Research on dynamic analysis of pipes conveying fluid has been abundant [1, 5, 20-22]. The knowledge gained in this modeling paradigm is readily applicable to many areas in applied mechanics research [23]; However, literature on the associated vibration control is quite limited. Liu, et al. [14] reported a feedforward control approach for active vibration suppression application. A considerable amount of research work has been done on the application of piezoelectric materials [4, 7, 8, 25, 26] in smart structures. Lin and Chu [11] examined the use of surface mounted piezoelectric actuator on flutter suppression of a cantilever tube conveying fluid. The control strategy developed in [12] was applied. The use of piezoelectric inertia actuators (PIA) for vibration control of smart structural systems was reported [6, 9, 10]. This study applies a piezoelectric inertia actuator for vibration suppression of a cantilever pipe by using an active control strategy. The mathematical model for the actuator dynamics is quite different from that of the surface mounted piezoelectric patch. The PIA has a distinct resonance frequency, at which its excitation is most effective. The resonance frequency can be adjusted according to the characteristics of the control system by externally attaching an appropriate mass.

The finite element method, with the Timoshenko beam theory being used, is applied to obtain the motion equations of a cantilever pipe and the attached piezoelectric inertia actuator. The optimal IMSC is applied for the design. This study reveals, for the first time, the strategy to determine the applicable in-

Paper submitted 08/31/11; revised 07/10/12; accepted 09/04/12. Author for correspondence: Yih-Hwang Lin (e-mail: yhl2@mail.ntou.edu.tw).
[1]Department of Mechanical and Mechatronic Engineering, National Taiwan Ocean University, Keelung, Taiwan, R.O.C.
[2]Twinhead International Corporation (Headquarter) Taipei, Taiwan, R.O.C.
[3]Department of Mechanical Engineering, Southern Taiwan University of Science and Technology, Tainan, Taiwan, R.O.C.
[4]Darfon Corporation (Headquarter), Taoyuan, Taiwan, R.O.C.

stability regions for the approach proposed by the IMSC pioneer developers, which exhibits severe control spillover problems for systems with complex modes. Stability of the system is dependent on how the left eigenvector is normalized. A systematic analysis will be performed by rotating the left eigenvector on the complex plane to define the instability region of the control system for the fluid-conveying pipe using a piezoelectric inertia actuator. To the best knowledge of the authors, the stability manipulation of the approach proposed by the IMSC pioneer developers has not been revealed in the literature and warrants a detailed analysis to further explore the stability characteristics of the complex control system for structural systems.

II. Model Development

Fig. 1 shows a fluid-conveying cantilever pipe with a piezoelectric inertia actuator attached at the free end. The finite element method, with the Timoshenko beam theory being applied, is employed to formulate the pipe and the fluid element matrices. The equations of motion for the fluid-conveying cantilever pipe, including the actuator dynamics, can be shown as:

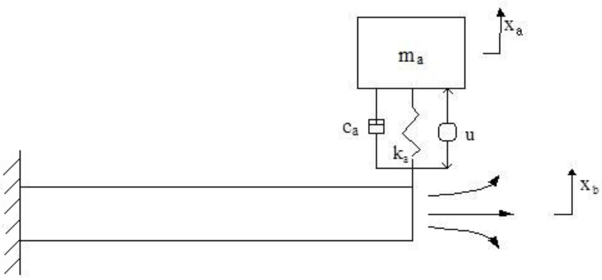

Fig. 1. A fluid-conveying pipe with a piezoelectric inertia actuator attached at the free end

$$\begin{pmatrix} [M] & 0 \\ \lfloor 0 \rfloor & m_a \end{pmatrix} \begin{Bmatrix} \{\ddot{x}_b\} \\ \ddot{x}_a \end{Bmatrix} + \begin{pmatrix} [C]+[c]^* & -c_a \lfloor N \rfloor^T \\ -c_a \lfloor N \rfloor & c_a \end{pmatrix} \begin{Bmatrix} \{\dot{x}_b\} \\ \dot{x}_a \end{Bmatrix} + \begin{pmatrix} [K]+[k]^* & -k_a \lfloor N \rfloor^T \\ -k_a \lfloor N \rfloor & k_a \end{pmatrix} \begin{Bmatrix} \{x_b\} \\ x_a \end{Bmatrix} = \begin{Bmatrix} -\lfloor N \rfloor^T u \\ u \end{Bmatrix} \tag{1}$$

where

$$[c]^* = c_a \lfloor N \rfloor^T \lfloor N \rfloor \tag{2}$$

$$[k]^* = k_a \lfloor N \rfloor^T \lfloor N \rfloor \tag{3}$$

and u is the active control input; $\lfloor N \rfloor$ represents the shape functions of the pipe element; $\{x_b\}$ and x_a are the displacements of the beam elements describing the pipe/fluid system and the PIA, respectively. m_a , c_a , and k_a are, respectively, the mass, damping, and stiffness of the PIA; [M], [C], and [K], denote the structural mass, damping, and stiffness matrices of the pipe/fluid system, respectively. The contributions of both the pipe and the flowing fluid are included to assemble the structural matrices. A detailed description of how to formulate those structural matrices can be found in [2, 24]. Equation (1) can be recast as:

$$\overline{M}\ddot{X} + \overline{C}\dot{X} + \overline{K}X = \overline{F} \tag{4}$$

where

$$\begin{aligned} \overline{M} &= \begin{pmatrix} [M] & 0 \\ \lfloor 0 \rfloor & m_a \end{pmatrix} \\ \overline{C} &= \begin{pmatrix} [C]+[c]^* & -c_a \lfloor N \rfloor^T \\ -c_a \lfloor N \rfloor & c_a \end{pmatrix} \\ \overline{K} &= \begin{pmatrix} [K]+[k]^* & -k_a \lfloor N \rfloor^T \\ -k_a \lfloor N \rfloor & k_a \end{pmatrix} \\ X &= \begin{Bmatrix} \{x_b\} \\ x_a \end{Bmatrix} \\ \overline{F} &= \begin{Bmatrix} -\lfloor N \rfloor^T u \\ u \end{Bmatrix}. \end{aligned} \tag{5}$$

To facilitate the control formulation, the governing equations of motion are expressed in the state space form, as shown below:

$$\dot{x} = Ax + B\overline{F}, \tag{6}$$

where

$$\begin{aligned} A &= \begin{bmatrix} -\overline{M}^{-1}\overline{C} & -\overline{M}^{-1}\overline{K} \\ I & 0 \end{bmatrix} \\ B &= \begin{bmatrix} \overline{M}^{-1} \\ 0 \end{bmatrix} \\ x &= \begin{Bmatrix} \dot{X} \\ X \end{Bmatrix}. \end{aligned} \tag{7}$$

Equation (6) represents a dynamical system possessing complex modes due to the gyroscopic effect from the fluid motion and the concentrated damper of the PIA. They can be decoupled by using the bi-orthogonality of the left and right eigenvectors. The system can thus be described in the modal space:

$$\dot{q}_s = \Lambda_s q_s + Q_{u_s} \ , \qquad s = 1 , 2 ,... , n, \tag{8}$$

where n is the number of modes of the system and

$$\Lambda_s = \begin{bmatrix} \sigma_s & \omega_s \\ -\omega_s & \sigma_s \end{bmatrix}, \tag{9}$$

and

$$q_s = [q_{2s-1} \;\; q_{2s}]^T, \; Q_{u_s} = L^T B \overline{F}. \tag{10}$$

in which σ_s and ω_s denote the real and imaginary parts, respectively, of the open loop eigenvalue of the s-th mode. The modal control input, Q_{u_s}, is related to the physical control input, $\overline{F}$, through a linear transformation using the left modal matrix, L, which is constructed using the left eigenvectors obtained by solving the adjoint eigenvalue problem. Note that there are infinite ways to normalize the left and right eigenvectors, and thus the elements within the left modal matrix are not unique. We consider optimal control in the modal space for the system examined. The modal control cost function for the steady state system response is defined as:

$$J_s = \int_0^\infty (q_s^T(t) q_s(t) + Q_{u_s}^T(t) E_s Q_{u_s}(t)) dt, \;\; s = 1, 2, ..., k, \tag{11}$$

where k is the number of modes controlled and E_s denotes the weighting matrix for the modal control input. The designer can make the selection of the weighting matrix based on the control requirement and available hardware. The optimal modal control input can be obtained as:

$$Q_{us} = -E_s^{-1} S_s q_s(t) = -K_s q_s(t), \quad \text{s=1,2, ..., k} \tag{12}$$

where K_s is the feedback gain matrix and S_s is the Riccati Matrix as obtained by solving the following nonlinear matrix equation:

$$S_s \Lambda_s + \Lambda_s^T S_s - S_s E_s^{-1} S_s + I = 0, \quad \text{s=1,2, ..., k} . \tag{13}$$

For the control of one complex mode using one actuator, the pioneer developers of the IMSC technique proposed the use of an infinite cost weight factor for $Q_{u_{2s-1}}$ such that it can be set to zero in the optimization process due to its infinite cost. By doing so, the weighting matrix can be shown as:

$$E_s^{-1} = \begin{bmatrix} 0 & 0 \\ 0 & E_{s22}^{-1} \end{bmatrix} \tag{14}$$

Note that initially one element of Q_{us} is forced to zero, but because of the control spillover, the original zero element will become non-zero. For each complex mode controlled, two modal states are used as feedback to synthesize the modal control input, which in turn is used to formulate the physical control input, u, through the left modal matrix. Control spillover exists in the process and has been taken into account in the analysis. The relation between the modal control input and the physical control input can be shown as:

$$\begin{pmatrix} Q_{u_{2s-1}}(t) \\ Q_{u_{2s}}(t) \end{pmatrix} = \begin{pmatrix} \eta_{2s-1} \\ \eta_{2s} \end{pmatrix} \overline{f}(t) \;\; , \;\; \text{s=1 ,2 , ... , n ,} \tag{15}$$

where $\overline{f}(t)$ is the physical control input; η_{2s-1} and η_{2s} are not unique due to the non-unique normalization process of the left and right eigenvectors. By substituting Eq. (14) into Eq. (13), we have successfully solved the resulting nonlinear Riccati matrix equation and the closed form solution can be written as:

$$S_s = \begin{bmatrix} S_{s11} & S_{s12} \\ S_{s21} & S_{s22} \end{bmatrix} \tag{16a}$$

in which

$$S_{s12} = S_{s21} = \frac{\sigma_s^2 - \omega_s^2 + \sqrt{(\sigma_s^2+\omega_s^2)(E_{s22}^{-1}+\sigma_s^2+\omega_s^2)} - \sigma_s\sqrt{E_{s22}^{-1} + 2\sigma_s^2 - 2\omega_s^2 + 2\sqrt{(\sigma_s^2+\omega_s^2)(E_{s22}^{-1}+\sigma_s^2+\omega_s^2)}}}{E_{s22}^{-1}\omega_s},$$

$$\begin{aligned} S_{s11} = {} & \frac{1}{E_{s22}^{-1}\omega_s^2}\Big\{E_{s22}^{-1}\sigma_s + 2\sigma_s^3 + 2\sigma_s\sqrt{(\sigma_s^2+\omega_s^2)(E_{s22}^{-1}+\sigma_s^2+\omega_s^2)} \\ & -\sigma_s^2\sqrt{E_{s22}^{-1} + 2\sigma_s^2 - 2\omega_s^2 + 2\sqrt{(\sigma_s^2+\omega_s^2)(E_{s22}^{-1}+\sigma_s^2+\omega_s^2)}} \\ & -\sqrt{(\sigma_s^2+\omega_s^2)(E_{s22}^{-1}+\sigma_s^2+\omega_s^2)\left[E_{s22}^{-1} + 2\left(\sigma_s^2 - \omega_s^2 + \sqrt{(\sigma_s^2+\omega_s^2)(E_{s22}^{-1}+\sigma_s^2+\omega_s^2)}\right)\right]}\Big\}, \end{aligned}$$

$$S_{s22} = \frac{2\sigma_s - \sqrt{E_{s22}^{-1} + 2\sigma_s^2 - 2\omega_s^2 + 2\sqrt{(\sigma_s^2+\omega_s^2)(E_{s22}^{-1}+\sigma_s^2+\omega_s^2)}}}{E_{s22}^{-1}}. \tag{16b}$$

The exact solution as given above alleviates the need to solve the notoriously stiff nonlinear Riccati equations, which are well known for the frequently encountered numerical difficulties and expensive computation.

III. NUMERICAL RESULTS

A total of eight finite elements is used to model the fluid-conveying pipe. An initial disturbance is given by applying a unit impact on the mid span of the pipe. The numerical data used for the simulation can be found in Table 1. The damping within the PIA is assumed negligible. The open loop poles of the second mode to be controlled are $-0.026 \pm 57.173i$. The corresponding gyroscopic damping due to the moving fluid results in 0.045% modal damping for the second mode of the fluid-conveying pipe, indicating a lightly damped open loop stable system. As is well known, further increase of the fluid speed will result in negative damping, leading to flutter instability in the second mode.

We first consider the case with a fixed control weight E_{s22}^{-1} = 10. For the system examined in this work, the second mode is dominant, and hence this mode is targeted to be controlled. Note that because of the severe control spillover, η_{2s-1}/η_{2s}, which is determined by how the complex left and right eigenvectors are normalized, will greatly affect the stability of the closed loop system. Consider the relation $l_s^T r_t = R_{st}$, where l_s and r_t denote the left and right eigenvectors, respectively, and R_{st} is in general a complex number. To obtain Eq. (8), l_s and r_t c a n b e

Table 1 Numerical data of the fluid-conveying pipe

Young's modulus	E = 68.9(10^9) Pa
Length of pipe	L = 3 m
Mass per unit length of the pipe	m_p = 0.3420 kg/m
Mass per unit length of the fluid	m_f = 0.0855 kg/m
Outside diameter of the pipe	d_o = 0.0254 m
Thickness of the pipe wall	t = 0.00165 m
Mass of the PIA	m_a = 0.0513 kg
Stiffness of the PIA	k_a = 165.0288 N/m

normalized by both multiplying a factor of $\sqrt{2/R_{st}}$. However, there are infinite ways to realize the normalization. The same normalization can be accomplished by using a complex number, $ze^{i\theta}$, to multiply l_s and to divide r_t simultaneously. Note that the magnitude 'z' has no effect on the outcome and it is the rotation angle 'θ' that solely makes the difference. The physical consequence of this operation can be considered as a rotation of the left eigenvector on the complex plane. For the independent modal space control of the fluid-conveying pipe with the pioneers' approach being applied, the following range of 'θ' is found to have resulted in an unstable closed loop system, including divergence and flutter instabilities:

$$0.717 \pm n\pi < \theta < 0.813 \pm n\pi, n = 0,1,2,... \qquad (17)$$

Note that the open loop system is stable in this analysis case, with the second mode eigenvalue being $-0.026 \pm 57.173i$. Fig. 2 illustrates the tip response of the fluid-conveying pipe.

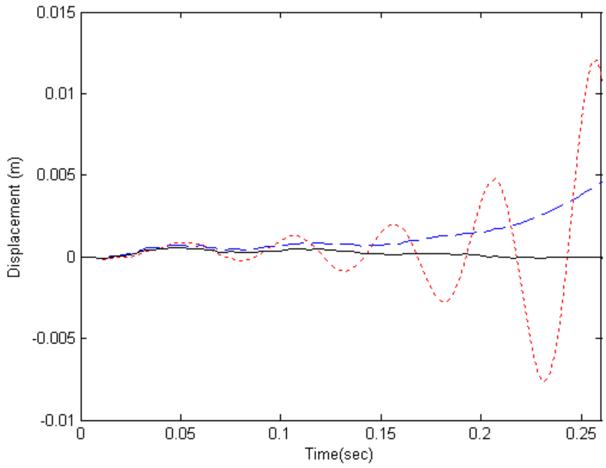

Fig. 2. Tip responses for different rotation angles of the left eigenvector with E_{s22}^{-1} being fixed.
……: $\theta = 0.81$, ____ : uncontrolled, − − −: $\theta = 0.73$.

As can be seen, the closed loop instability can be either of the flutter type or of the divergence type, depending on how the left eigenvector is normalized. The angle of rotation, 'θ', of the left eigenvector on the complex plane plays a crucial role on the stability of the smart system. For $\theta = 0.73$, the closed loop poles are (23.267, -29.073), showing a divergence instability, whereas for $\theta = 0.81$, the closed loop poles are $0.412 \pm 137.640i$, representing a flutter instability. Fig. 3 illustrates the variation of the second closed loop pole as the angle of rotation, 'θ', changes.

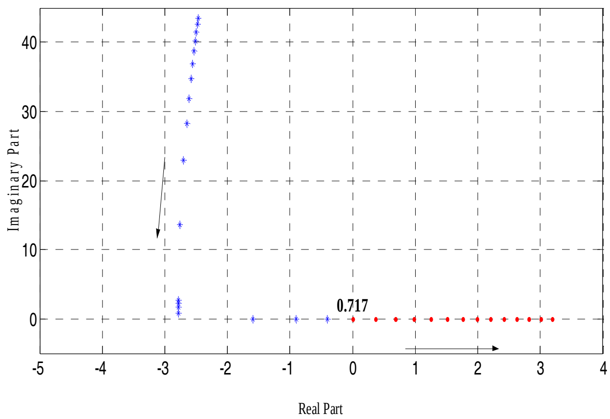

Fig. 3. The second mode root loci in the vicinity of the divergence instability as the rotation angle, θ, of the left eigenvector changes while the modal control weight E_{s22}^{-1} remains fixed.

The critical angle of rotation for divergence can be clearly seen when the root passes the origin of complex plane. Similarly, in Fig. 4, the second closed loop pole can be seen to come across the imaginary axis as the angle of rotation reaches 0.813.

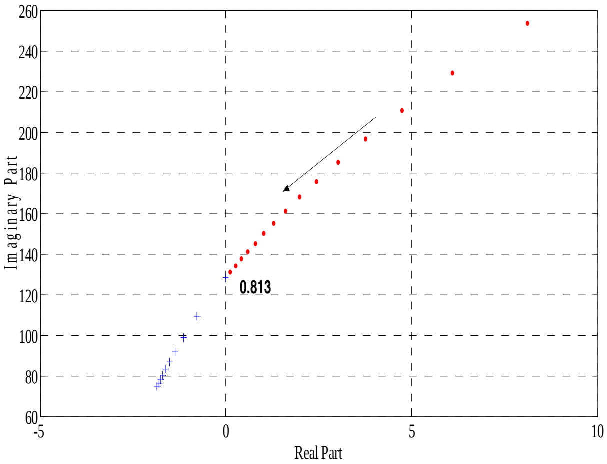

Fig. 4. The second mode root loci in the vicinity of the flutter instability as the rotation angle, θ, of the left eigenvector changes while the modal control weight E_{s22}^{-1} remains fixed.

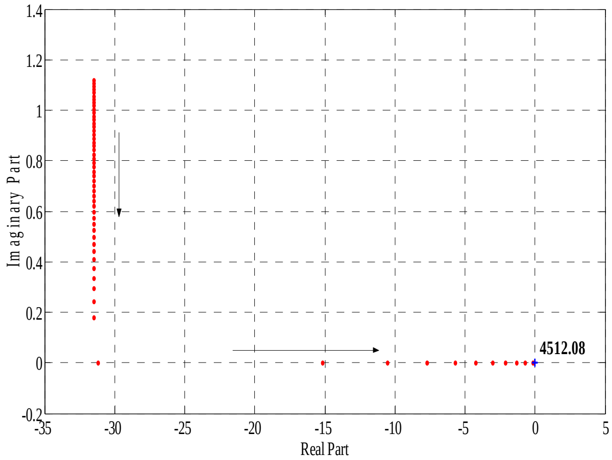

Fig. 6. The second mode root loci in the vicinity of the lower bound divergence instability as the modal control weight E_{s22}^{-1} changes while the left eigenvector remains fixed.

The effect of the control weight E_{s22}^{-1} on the stability of the system is also examined with the ratio η_{2s-1}/η_{2s} being fixed. The eigenvectors l_s and r_t are both multiplied by the baseline complex number, $\sqrt{2/R_{st}}$, to satisfy the normalization requirement. The following range of the control weight can be shown to render the system unstable with divergence instability:

$$4512.080 < E_{s22}^{-1} < 9.861(10^6) \tag{18}$$

Fig. 5 shows the tip response of the fluid-conveying pipe with $E_{s22}^{-1} = 10000$. It can be seen the instability is of the divergence type. Figures 6 and 7 depict the trace of the second mode as the control weight E_{s22}^{-1} changes.

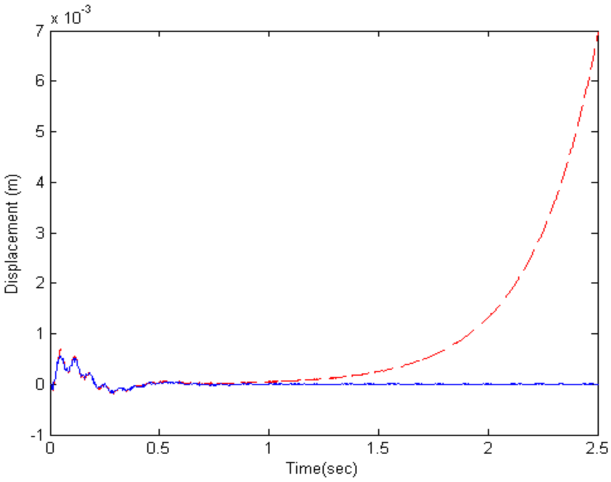

Fig. 5. The controlled and uncontrolled tip responses with a fixed baseline left eigenvector, illustrating divergence instability.
----- : $E_{s22}^{-1} = 10000$, ____ : uncontrolled

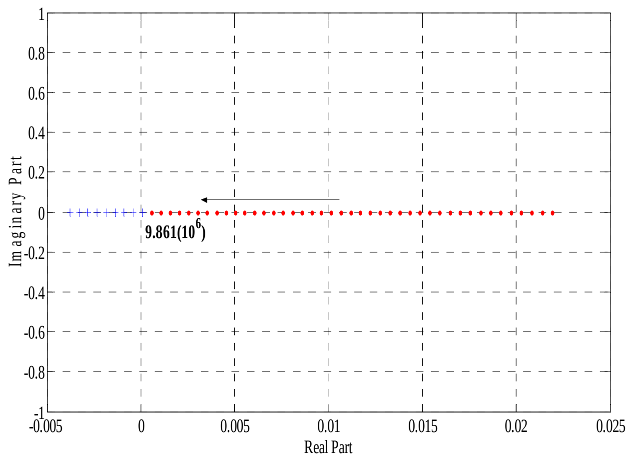

Fig. 7. The second mode root loci in the vicinity of the upper bound divergence instability as the modal control weight E_{s22}^{-1} changes while the left eigenvector remains fixed.

IV. CONCLUSIONS

In this study, stability analysis of the approach proposed by the pioneer developers of the IMSC technique has been presented and illustrated by a numerical example concerning active vibration control of a fluid-conveying pipe using a piezoelectric inertia actuator. The approach can easily lead to an unstable system due to severe control spillover within the complex mode controlled. The analyst has no prior knowledge of the closed loop stability of the system because there are infinite ways to satisfy the requirement of the eigenvector normalization. For the first time in the literature, we have revealed the interesting stability characteristics of the control system with the IMSC technique used by rotating the left eigenvector in the complex plane while realizing the normalization requirement. The catastrophic instability design, even for open loop stable systems, can thus be circumvented.

ACKNOWLEDGEMENT

The authors are grateful to the National Science Council, NSC, Taiwan, Republic of China, for financial support under the contract NSC97-2221-E-019-055-MY3 and the National Center for High-performance Computing for computer time and facilities.

REFERENCES

1. Chen, S.-S., "Flow-induced vibration of circular cylindrical structures. Part I: Stationary fluids and parallel flow," *Shock and Vibration Digest,* Vol. 9, pp. 25-38 (1977).
2. Chu, C.-L., and Lin, Y.-H., "Finite element analysis of fluid-conveying Timoshenko pipes," *Shock and Vibration,* Vol. 2, No. 3, pp. 247-255 (1995).
3. Chu, C.-L., Wu, B.-S., and Lin, Y.-H., "An experimental study on active micro-vibration suppression of a flexible beam mounted on an elastic base," *Measurement Science and Technology,* Vol. 18, pp. 1823-1830 (2007).
4. Gibbs, G. P., and Fuller, C. R., "Experiments on active control of vibration power flow using piezoceramic actuators/sensors," *American Institute Aeronautics and Astronautics Journal,* Vol. 30, No. 2, pp. 457-463 (1992).
5. Housner, G. W., "Bending vibrations of a pipe when liquid flows through it," *Journal of Applied Mechanics,* Vol. 19, pp. 205-208 (1952).
6. Lesieutre, G. A., Rusovici, R., Koopmann, G. H., and Dosch, J. J., "Modelling and characterization of a piezoceramic inertial actuator," *Journal of Sound and Vibration,* Vol. 261, No. 1, pp. 93-107 (2003)
7. Liao, C.-Y., and Sung, C.-K., "Vibration suppression of flexible linkage mechanisms using piezoelectric sensors and actuators," *Journal of Intelligent Material Systems and Structures,* Vol. 2, pp. 177-197 (1991)
8. Li, F.-M., Kishimoto, K., Wang, Y.-S., Chen, Z.-B., and Huang, W.-H., "Vibration control of beams with active constrained layer damping," *Smart Materials and Structures,* Vol. 17, No. 6, pp. 065036 (2008).
9. Ling, S.-F., and Xie, Y., "Detecting mechanical impedance of structures using the sensing capability of a piezoceramic inertial actuator," *Sensors and Actuators A,* Vol. 93, pp. 243-249 (2001).
10. Ling, S.-F., and Xie, Y., "Monitoring structural integrity using a piezoelectric inertial actuator cum sensor," *Journal of Sound and Vibration,* Vol. 247, No. 4, pp. 731-737 (2001).
11. Lin, Y.-H., and Chu, C.-L., "Active Flutter Control of a Cantilever Tube Conveying Fluid using Piezoelectric Actuators," *Journal of Sound and Vibration,* Vol. 96, No. 1, pp. 97-105 (1996).
12. Lin, Y.-H., and Chu, C.-L., "A new design for independent modal space control of general dynamic systems," *Journal of Sound and Vibration,* Vol. 180, No. 2, pp. 351-361(1995).
13. Lin, Y.-H., Huang, R.-C., and Chu, C.-L., "Optimal modal vibration suppression of a fluid-conveying pipe with a divergent mode," *Journal of Sound and Vibration,* Vol. 271, pp. 577–597 (2004).
14. Liu, C.-C., Li, F.-M., Fang, B., Zhao, Y., and Huang, W.-H., "Active control of power flow transmission in finite connected plate," *Journal of Sound and Vibration,* Vol. 329, No. 20, pp. 4124–4135 (2010).
15. Meirovitch, L., and Baruh, H., "Optimal control of damped flexible gyroscopic systems," *Journal of Guidance and Control,* Vol. 4, No. 2, pp. 157-163 (1981).
16. Meirovitch, L., and Baruh, H., "Robustness of the independent modal-space control method," *Journal of Guidance and Control,* Vol. 6, No. 1, pp. 20-25 (1983).
17. Meirovitch, L., and Ghosh, D., "Control of flutter in bridges," *Journal of Engineering Mechanics , ASCE,* Vol. 113, No. 5, pp. 720-736 (1987).
18. Meirovitch, L., Baruh, H., and Öz, H., "A comparison of control techniques for large flexible systems," *Journal of Guidance and Control,* Vol. 6, No. 4, pp. 302-310 (1983).
19. Öz, H., and Meirovitch, L., "Optimal modal-space control of flexible gyroscopic systems," *Journal of Guidance and Control,* Vol. 3, No. 3, pp. 218-226 (1980).
20. Paidoussis, M. P., and Issid, N. T., "Dynamic stability of pipes conveying fluid," *Journal of Sound and Vibration,* Vol. 33, pp. 267-294 (1974).
21. Paidoussis, M. P., "Flow-induced instability of pipes conveying fluid," *Applied Mechanics Reviews,* Vol. 40, pp. 163-175 (1987).
22. Paidoussis, M. P., "Flutter of conservative systems of pipes conveying incompressible fluid," *The Journal of Mechanical Engineering Science,* Vol. 17, pp. 19-25 (1975).
23. Paidoussis, M. P., "The canonical problem of the fluid-conveying pipe and radiation of the knowledge gained to other dynamics problems across Applied Mechanics," *Journal of Sound and Vibration,* Vol. 310, No. 3, pp. 462-492 (2008).
24. Pramila, A., Laukkanen, J., and Liukkonen, S., "Dynamics and stability of short fluid-conveying Timoshenko element pipes," *Journal of Sound and Vibration,* Vol. 144, No. 3, pp. 421-425 (1991).
25. Rao, S. S., and Sunar, M., "Analysis of distributed thermopiezoelectric sensors and actuators in advanced intelligent structures," *American Institute Aeronautics and Astronautics Journal,* Vol. 31, No. 7, pp. 1280-1286 (1993).
26. Tzou, H.- S., and Tseng, C.-I., "Distributed piezoelectric sensor/actuator design for dynamic measurement/control of distributed parameter systems: a piezoelectric finite element approach," *Journal of Sound and Vibration,* Vol. 138, No. 1, pp. 17-34 (1990).